Cathodoluminescence and electrical study of vertical GaN-on-GaN Schottky diodes with dislocation clusters

Thi Huong Ngo, Rémi Comyn, Eric Frayssinet, Hyonju Chauveau, Sébastien Chenot, Benjamin Damilano, Florian Tendille, Bernard Beaumont, Jean-Pierre Faurie, Nabil Nahas, et al.

Cathodoluminescence and electrical study of vertical GaN-on-GaN Schottky diodes with dislocation clusters

Thi Huong Ngo, Rémi Comyn, Eric Frayssinet, Hyonju Chauveau, Sébastien Chenot, Benjamin Damilano, Florian Tendille, Bernard Beaumont, Jean-Pierre Faurie, Nabil Nahas, et al.

Version of Record: https://www.sciencedirect.com/science/article/pii/S0022024820304346
Manuscript_ed76d7654cd964f5c1f6f8e8e0075b71

Cathodoluminescence and electrical study of vertical GaN-on-GaN Schottky diodes with dislocation clusters

Thi Huong Ngo[1], Rémi Comyn[1], Eric Frayssinet[1], Hyonju Chauveau[2], Sébastien Chenot[1], Benjamin Damilano[1], Florian Tendille[2], Bernard Beaumont[2], Jean-Pierre Faurie[2], Nabil Nahas[2], Yvon Cordier[1*]*

1-Université Côte d'Azur, CNRS, CRHEA, rue Bernard Grégory, 06560 Valbonne, France

2-Saint Gobain Lumilog, 2720 Chemin Saint Bernard, 06220, Vallauris, France

Corresponding author e-mail: thi.huong.ngo@crhea.cnrs.fr; yvon.cordier@crhea.cnrs.fr

Electrical properties of vertical Schottky diodes fabricated on GaN regrown on hydride vapor phase epitaxy GaN substrates are investigated. The deposition of Ni frames makes it possible to designate the dislocation locations by cathodoluminescence before the fabrication of diodes. Since the distribution of dislocations is inhomogeneous and arranged into clusters over the GaN substrates, diodes made on either areas free of dislocation-clusters or areas with dislocation-clusters have been studied. Both forward and reverse characteristics of diodes fabricated on GaN with different doping levels and dislocation densities have been investigated. It is shown that the reverse leakage is not sensitive to the presence of dislocation clusters. On the other hand, there is a dispersion of reverse leakage which increases in diodes grown on substrates having larger mean dislocation density. The results also demonstrate that a critical maximum distance of around 100 µm between active defects triggers larger reverse leakage currents.

Keywords: Gallium Nitrides, Schottky diodes, Dislocations, Cathodoluminescence, Reverse leakage current, Variable-range-hopping mechanism.

1. Introduction

The high saturation electron velocity and the high critical electric field of GaN offer advantages to alternative conventional Si-based electronics for manufacturing high power, high frequency devices, and circuits.[1],[2] Moreover, the growing GaN on various substrates

by epitaxial technologies leads to significant progress in terms of material and device production. However, when GaN is grown on foreign substrates such as sapphire, silicon, and silicon carbide, large lattice mismatch and thermal expansion coefficient mismatch induce high strain and high defect density (>>10^7 cm^{-2}) in the GaN epi-layers.[3],[4] The high defect density limits the performance and reliability of GaN-based devices. Bulk GaN is the ideal substrate for fabrication of high performance devices owing to the matching lattice parameter and thermal expansion coefficient.[5-7] Fabricating power electronic devices[8,9] and optoelectronic components[10,11] on a bulk GaN substrate advantageously combines the absence of strain, structural defects, and the thermal barrier. However, this ideal continues to face the difficulties of synthesizing large substrates. For this reason, alternative solutions such as self-supported GaN substrates are being developed on an industrial scale. In this technique, GaN substrates are developed by thickening nucleated GaN on sapphire substrates with diameters ranging from 50 to 100 mm.[12] This technique makes it possible to reduce the average density of dislocations from a few 10^8 cm^{-2} to less than 10^7 cm^{-2}. However, it appears that the dislocations are not fully eliminated but accumulate partially in clusters.[13,14]

Although the non-radiative recombination at dislocations can be highlighted by cathodoluminescence (CL), the electrical behavior of these clusters of dislocations is still under debate. Attempts to correlate parameters such as surface morphology, dislocation density, residual doping, and electrical behavior have been carried out in the last years. They have shown the complex nature of the problem.[15-20] For instance, some studies pointed out the detrimental role of carbon in the generation of defects related to leakage paths,[18,19] while others mentioned particular dislocations as responsible for electrical leakage.[20] Elucidating the relationship between electrical activity and structure defects is essential to developing GaN substrates for applications such as light-emitting diodes (LEDs) and laser diodes (LDs) for lighting, p-n or Schottky high voltage rectifying diodes and power switching transistors.

In the present study, the correlation between electrical properties of vertical GaN Schottky diodes and dislocations of hybrid vapor phase epitaxy (HVPE) GaN substrates is investigated. For this purpose, the dislocation density in the GaN substrates is estimated via X-ray diffraction and CL observation before the growth of lightly n-doped GaN films. Then Ni frames have been deposited to designate areas where Schottky diodes will be fabricated. A second cathodoluminescence observation is performed to examine the density and arrangement of dislocations of the GaN epi-layer within Ni frames before diode fabrication. Then capacitance-voltage (C-V) measurements assess the uniformity of doping and current-voltage (I-V) characterizations evaluate the forward and reverse bias characteristics of the diodes. In the first step, it is shown that the I-V behavior of the diodes is comparable to that of diodes previously reported in the literature on low defect density materials.[9,21] Furthermore, it is shown that the reverse leakage current is not sensitive to the presence of dislocation clusters; and we find similar electrical characteristics for diodes on GaN substrates having different dislocation density but the same the doping level. On the other hand, the reverse I-V measurements of diodes show a dispersion of leakage over the substrates. The more substantial variation is found on substrates of larger mean dislocation density. Also, a critical distance between the active defects that trigger larger reverse leakage currents is estimated at around 100 µm which represents an active defect density around 10^4 cm^{-2}.

2. Sample growth and diode fabrication

2. 1. Growth structure and inspection of crystal quality

For this study, 3 µm thick GaN films were grown on three 2-inch HVPE GaN substrates by MOVPE in a close-coupled showerhead Aixtron reactor.[22] Ammonia, trimethylgallium, and hydrogen carrier gas were used to grow the films at 1020 °C with a growth rate of 2 $\mu m.h^{-1}$. Diluted silane was added to the vapor phase in order to dope the GaN films.

Table 1. Structure parameters of the A, B, and C samples.

Sample	**A**	**B**	**C**
Off-cut angle at the center [°]	0.53	0.59	0.57
Off cut variation across the wafer	± 0.05	± 0.05	± 0.05
Substrate XRD FWHM $GaN_{(002)}$ [arcsec]	109	86	100
Substrate XRD FWHM $GaN_{(201)}$ [arcsec]	190	127	156
Dislocations Density estimated by CL [$x10^6$ cm^{-2}]	10	5.5	8.5
Root Mean Square Roughness [nm]	0.1	0.1	0.1
Doping of n-GaN [$x10^{16}$ cm^{-3}]	8.1 ± 0.2	8.4 ± 0.3	5.5 ± 0.2

Table I summarizes the structure parameters of the GaN substrates and the GaN epi-layers for all samples. The A, B, and C samples present similar *c-axis* off-cut angles ranging from 0.53° to 0.59°. Sample A and sample B were grown in the same epitaxy run and on substrates having different crystal quality. The latter is estimated via the full width at half maximum (FWHM) of symmetric (002) and asymmetric (201) X-ray diffraction (XRD) omega scan peaks which depend on the dislocation density. No noticeable change of the FWHMs of XRD peaks was observed after the MOVPE growth.

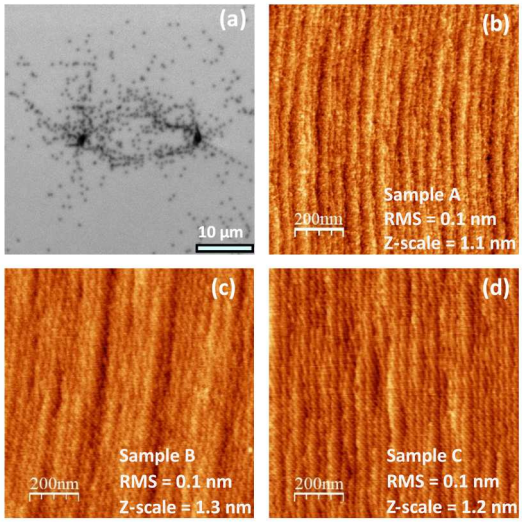

***Figure 1**: (a) A cathodoluminescence image of two clusters on a GaN substrate. (b), (c), (d) Surface morphology analysed by atomic force microscopy in a scan range of 2x2 µm² for the A, B and C samples, respectively. The root mean square roughness was estimated to about 0.1 nm for all the samples.*

The CL images were recorded at room temperature using an acceleration voltage of 10 kV and a magnification of 500x or 1000x. By inspection of 15 CL images for each sample, the dislocation density is found to be 5-10 x 10^6 cm^{-2} in areas of 187 500 µm², as listed in Table I. Even if a part of dislocations may not be revealed and counted by CL due to a lack of resolution or of luminescence contrast,[23] the fact that densities reported in Table 1 vary in a similar way as the XRD (002) and (201) line widths confirms the interest of this method. Figure 1(a) illustrates a CL image of a dislocation cluster. The mean dislocation density in such a cluster has been estimated to be 2 x 10^8 cm^{-2} in the 100 µm² surrounding area by atomic force microscopy; see supplementary data for details. If we exclude these areas the mean dislocation density is estimated to be 3.5 to 8 x 10^6 cm^{-2} depending to the sample. Figures 1(b,c,d) show the surface morphology of as-grown GaN films determined by tapping mode atomic force microscopy with values of root mean square (RMS) roughness around 0.1 nm for the scan range of 2x2 μm^2. A clear feature of molecular monolayer steps is observed without the presence of wide pits or hillocks related to dislocations. These surface steps and terraces are very similar to those reported in Ref. 9 for GaN grown on a substrate having an extremely low defect density of 5x10^4 cm^{-2}. The above results confirm that we obtained low-defect-density GaN epilayers with smooth surface morphology by using homoepitaxial growth.

2.2. Frame and diode fabrication

Standard ultraviolet-photolithography, e-beam evaporation, lift-off, and reactive ion etching (RIE) are used for the fabrication of Ni frames and the SBDs, as described in figure 2. On the front side of the GaN wafer, 40 nm thick Ni frames are first deposited (Figs. 2-a,b). Then CL observations are performed for the GaN layer located inside the rectangular Ni frames (Fig. 2-c). Before fabrication of the metal contacts, the virtual locations of diodes are determined within the Ni frames and shown by using blue circles, as in Fig. 2(c). The diodes are named as 200 µm, 100 µm, 50 µm (high) and 50 µm (low) based on their diameters and their positions.

This technique allows us to inspect the arrangement of dislocations in the GaN layers before the fabrication of metal contacts.

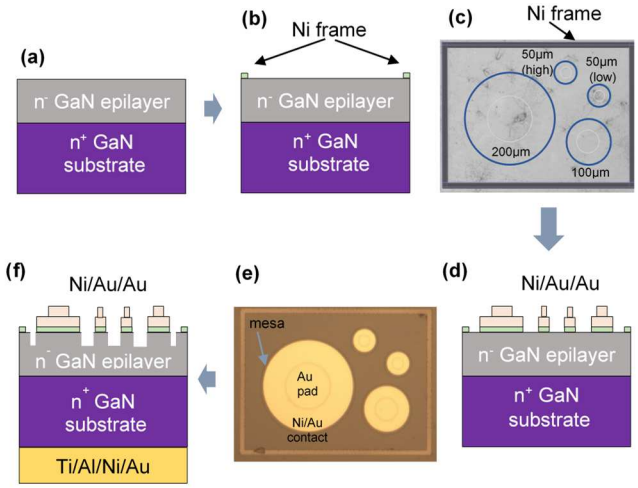

***Figure 2**: Schematic diagram of the device processing.*

For the proposed high quality Schottky diodes, a clean contact between metal and semiconductor is required. Therefore, the Ni/Au contacts are evaporated before making the mesa isolation in order to limit as much as possible parasitic contaminations at the interface between Ni and the GaN epilayer. Inside the Ni frames, the circular Ni/Au (20/200 nm) Schottky contacts are deposited, followed by an additional 200 nm Au pad at the center of the diodes to facilitate the electrical contact with needle probes (Fig. 2-d). Then diodes are isolated by mesa etching with an etching depth of 400 nm using $Cl_2/Ar/CH_4$ based RIE. The mesa etching was performed using an additional lithography step with another mask-set. In this mask-set each mesa pattern is wider than the Schottky contact by 10 µm. An optical microscope image of one Ni frame shown in Fig. 2(e) expresses well-formed Schottky diodes after the whole device fabrication. Finally, Ti/Al/Ni/Au (30/180/40/200 nm) stacks are deposited at the backside of the n^+-GaN substrate to make Ohmic contacts (Fig. 2-f). The electrical performances of the diodes are evaluated by the capacitance-voltage (C-V) and current-voltage (I-V) measurements using an Agilent 4284A LCR meter and a Keithley 2400 SourceMeter, respectively.

3. Results and discussions

One of the critical factors that determine the conduction mechanism of metal-n-type semiconductors is the doping level of the semiconductors. For an intermediate and highly doped semiconductor, the depletion region is sufficiently thin, and the barrier height is narrow, for electrons to tunnel through the barrier potential into the metal by field-thermionic emission or field emission.[24] In order to avoid this, the doping concentration of our GaN epi-layers is targeted at a level below 10^{17} cm^{-3}. The donor concentrations in the GaN layers are estimated from the slope of $1/C^2$ versus reverse bias at the frequency f = 100 kHz. Figure 3(a) shows the C-V curves and $1/C^2$-V profiles for 200 µm diodes located along the radius of sample A. The mean donor concentration of 8 x 10^{16} cm^{-3} with a good uniformity over the radius of the GaN wafer is reported in Fig. 3(b). Similar behaviors have been obtained on the other samples, and the mean doping levels are listed in Table I. The doping level in sample B is similar to that of sample A whereas it is noticeably lower in sample C.

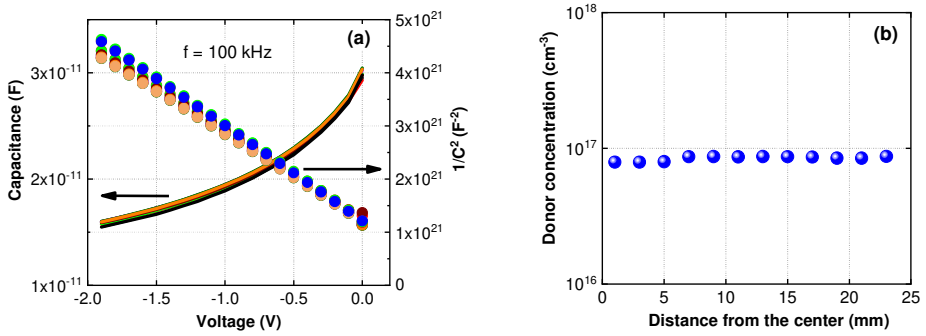

***Figure 3**: (a) Solid lines represent capacitance-voltage curves and dotted lines show the $1/C^2$ – voltage profiles. The measurement is recorded at the frequency f = 100 kHz. (b) Donor concentration profile of 200 µm diodes along the radius of sample A.*

Figure 4 (a) shows the forward I-V characteristics recorded for diodes located within one Ni frame of sample B. In order to avoid degradation of the devices, the forward injection current density is limited to 2000 $A.cm^{-2}$. The behavior noticed at forward bias lower than 0.2 V may imply some leakages, but the extremely low current level makes further study in this bias range difficult. When the forward voltage is in the range of 0.2-0.6 V, the I-V curves of all

diodes exhibit the superimposed exponential dependences. This independence of current density with the diode size confirms that the leakage occurs under the Ni/Au contacts only and that there is no noticeable leakage at the diode periphery. When the forward bias is beyond 0.6 V, the increase of current density is limited by the series resistance.

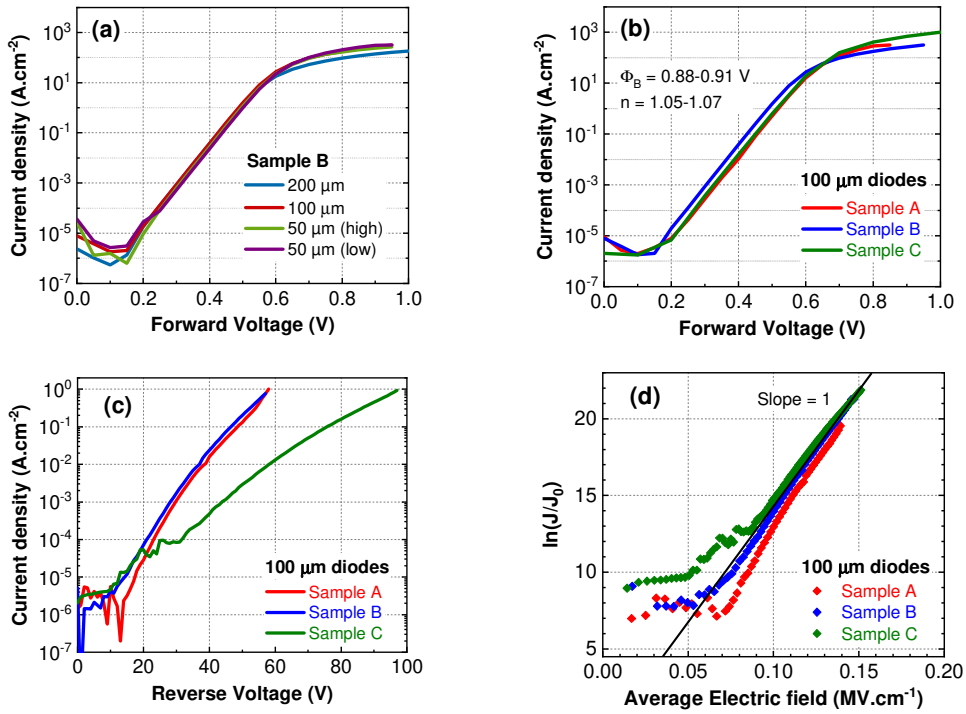

Figure 4: *(a) Semi-logarithmic plots of forward bias current-voltage characteristics of 50 µm 100 µm, 200 µm diodes located within one Ni frame of sample B. The superimposed curves demonstrate the absence of leakage at the diode peripheries. (b) Forward bias current-voltage characteristics of 100 µm diodes on A, B, and C samples. The ranges of barrier height Φ_B and ideality factor n are also given. (c) Plot of reverse injection current-voltage characterizations of the 100 µm diodes. (d) Plot of ln(J/J₀) as a function of the average electric field E in the depletion region of the 100 µm diodes.*

Figure 4 (b) shows a comparison of the forward I-V characteristics recorded for 100 µm diodes of A, B, and C samples. The I-V curves of all diodes exhibit the same exponential dependence when the voltage increases from 0.2 V to 0.6 V. As the n^--GaN layers are lightly doped with doping concentration lower than 10^{17} cm^{-3}, the exponential part of the I-V curves can be expressed by the thermionic emission in the following equation:[24,25]

$$J = A^* T^2 \exp\left(-\frac{q\emptyset_B}{kT}\right)\left[\exp\left(\frac{qV}{nkT}\right)\right] \quad (1)$$

where A^* is the Richardson constant of GaN, T represents the temperature, q is the elementary charge, Φ_B accounts for the barrier height of the Ni/GaN Schottky contact, k is the Boltzmann constant, V represents the applied voltage, n indicates the ideality factor. The barrier height and ideality factor are extracted from the intercept and the slope of ln(I)-V dependence, respectively. The diode barrier heights are 0.88-0.91 V which is in the high range of reported values in the literature on Ni/GaN Schottky diodes.[9,26-28] The ideality factors are nearly unity (1.05-1.07) for the studied diodes.

The reverse I-V curves of the same diodes are illustrated in figure 4(c). The reverse current density is limited to 1 A.cm^{-2} to avoid severe damage to the devices. When the reverse bias goes beyond 10 V, the leakage current increases almost exponentially with the reverse voltage at a rate that cannot be accounted for by the thermionic emission. The diodes of A and B samples grown with the same doping level show the same reverse I-V characteristics. A significant drop of the reverse current is found in sample C when the doping level is reduced to 5.5 x 10^{16} cm^{-3}, and crystal quality is intermediate. The leakage of sample C is similar to what was reported in Ref. 21 for Ni/GaN Schottky diodes fabricated on GaN layers grown on Sapphire but doped with a noticeably lower donor concentration of 1.8 x 10^{16} cm^{-3}. This illustrates how the better crystal quality of the GaN substrate can mitigate the effect of a larger donor concentration on the resulting leakage.

To explain the mechanisms accounting for the increase of leakage current with the reverse bias, we inspect an evolution of ln(J/J$_0$) with the average electric field E in the depletion region. The values of the average electric field E and the zero-field current density J_0 are determined from the following equations

$$E = \sqrt{\frac{2qN_d(\Phi_b - V)}{\varepsilon_r \varepsilon_0}} \quad (2)$$

$$J_0 = A^* T^2 \exp\left(-\frac{q\Phi_b}{kT}\right) \quad (3)$$

where N_d is the donor concentration, ε_r, ε_0 are the GaN relative and vacuum permittivity, respectively.

As shown in Fig. 4(d), for the electric field lower than 0.05 MV.cm^{-1} corresponding to the reverse bias below 10 V, the current is almost independent of the bias. When the electric field is increased, it induces a reduction of barrier height and hence causes the early stage of leakage current rise. Another mechanism that can contribute to the low-bias leakage current is the recombination of electron-holes at defect states. Free electrons can recombine non-radiatively with captured holes, at interface states or defects within the depletion region, due to the Shockley Read Hall (SRH) mechanism.[29,30] So, the combination of barrier lowering and SRH non-radiative recombination causes the leakage current for low electric field conditions. When the electric field is beyond 0.1 MV.cm^{-1}, the ln(J/J$_0$)-E plots follow linear dependences with slopes equal to 1. It demonstrates tunneling of electrons through the barrier into the semiconductor via the trap-assisted tunneling process[31] or the variable-range-hopping (VRH).[21,30] Well fitted curves of experimental data with the VRH model have been demonstrated for good quality GaN-on-GaN diodes.[15,32]

In the present GaN substrates, dislocations concentrate randomly into clusters at some locations, as illustrated in Figs. 5(a, b). The blue circles expressing locations of Schottky diodes indicate that the diodes are fabricated either on areas free of dislocation-clusters or areas containing these clusters. To be more precise, most diodes of frame 1 are made on GaN containing dislocation-clusters, except for the case of 50 µm (low) diode. Within frame 2, only the 200 µm diode is fabricated on dislocation-clusters while the other diodes are located on areas free of dislocation-clusters. The reverse I-V curves of those diodes are illustrated in Figs. 5(c,d). Within frame 1, despite the presence or absence of dislocation-clusters at the locations of diodes, the reverse I-V characteristics of the diodes superimpose until they reach a breakdown. This breakdown is caused by a hard breakdown at the periphery of the diodes (inset of Fig. 5(c)) when the reverse leakage current density is 1-10 A.cm^{-2}, in the same range

of the one reported for p-n diodes.[33] It is due to the large electric field located at the edge of the Schottky contact in the absence of a field plate.[34] The independence of reverse bias current density with diode size indicates that the leakage occurs under the whole surface of the diode until the hard breakdown regime is reached. In contrast with the superimposed curves of the diodes of frame 1, the reverse I-V characteristics of diodes within frame 2 present a dispersion with the lowest leakage is found for the 50 µm diodes. Moreover, the 200 µm diode located on dislocation-clusters exhibits a lower leakage current than the 100 µm diode locating on an area free of dislocation-clusters does. These observations evidence an independence of the reverse leakage current on the presence of dislocation-clusters.

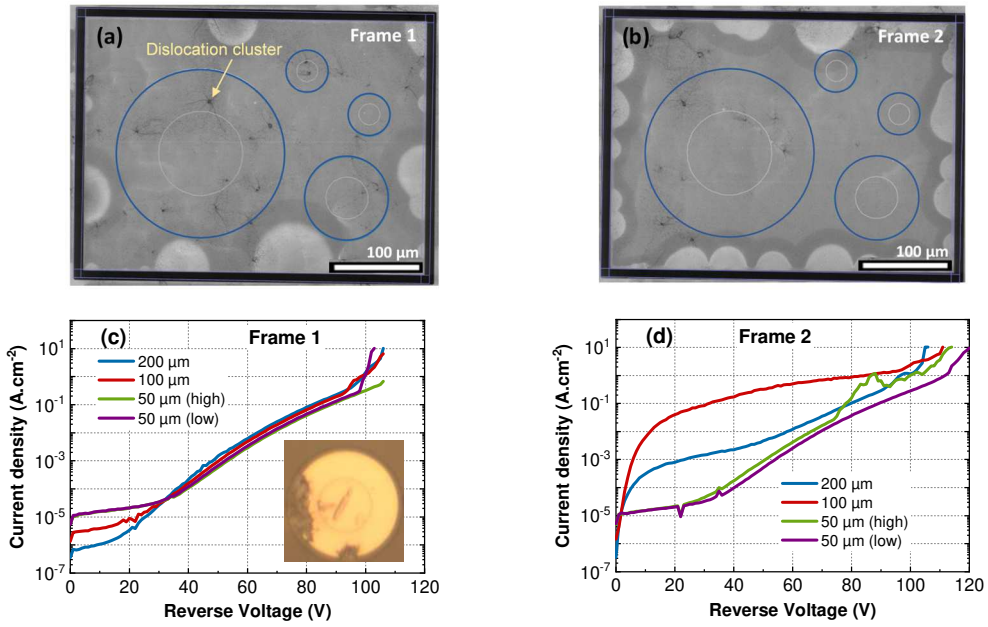

Figure 5: *(a), (b) Cathodoluminescence images of GaN layer within Ni frames of sample C: blue circles represent locations of the diodes. (c), (d) Plots of reverse current-voltage characteristics of diodes fabricated within the frame 1 and frame 2, respectively. The inset of figure (c) shows an optical microscope image of the 100 µm diode damaged by the hard breakdown.*

Results shown in Fig. 4 and Fig. 5 manifest that, despite different mean crystal quality substrates, it is possible to find diodes with similar forward and reverse electrical characteristics, the latter being sensitive to the GaN doping level. On the other hand, some diodes show reverse leakage and hard breakdown behavior independent of the presence of

dislocations-clusters while other diodes reveal some dispersion of the reverse leakage, which is not revealed by the crystal quality assessment of CL microscopy.

To further investigate the possible origin of leakage variations, statistic distributions of reverse breakdown voltage defined at a current density of 1 mA.cm^{-2} are studied on a total of 280 diodes with different size and located over the radius of the samples. As seen in Fig. 6, diodes of sample C have the highest reverse breakdown voltage which implies the lowest leakage current. Notice that this sample has an intermediate dislocation density and the lowest donor concentration (Table I). The A and B samples have similar donor concentrations but different crystal quality showing the same maximum reverse bias of about 30 V. It confirms similar leakage current in the best diodes of these two samples. However, less numerous leaky diodes are found for sample B which has a lower mean dislocation density.

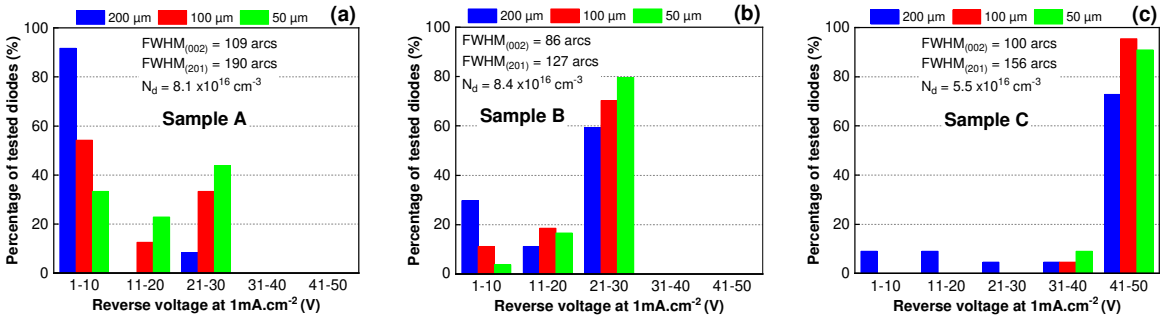

Figure 6: *(a), (b), (c) Histogram of percentage of tested diodes against the reverse breakdown voltage at the current density of 1 mA.cm^{-2} for diodes fabricated on the samples A, B and C, respectively. XRD data and donor concentrations are also recalled.*

A size dependence of leakage is found. While the 50 µm and 100 µm diodes denote similar reverse breakdown voltages, a noticeable dispersion appears for 200 µm diodes. To be more precise, most 200 µm diodes on sample A are significantly leaky whereas 60-70 % of 200 µm diodes of samples B and C exhibit a low leakage level. In these statistics, as the distances between diodes within a frame are relatively small, on the order of 50-100 µm, the influences of the diode sizes and distances may be considered in the same way. These observations demonstrate that the mean critical distance between the active defects that trigger reverse leakage superior to the ordinary ones is about 100 µm. That is to say, the density of these

distinctive active defects is estimated to 10^4 cm^{-2}. These distinctive active defects might be present either inside or outside clusters of dislocations, hence their probabilities to cause a noticeable leakage for a diode is random. The location of these distinctive active defects and the physical mechanism of the leakage conduction through them remains to be clarified with other characterizations like Electron or Optical beam induced current (EBIC or OBIC) techniques.[35,36]

4. Conclusion

In summary, an investigation of influences of dislocation density and their arrangement on electrical properties of vertical Schottky diodes fabricated on HVPE GaN substrates has been undertaken. The barrier heights, ideality factors, and reverse currents are comparable to those reported in the literature and indicate that our diodes are good quality devices with reverse leakage governed by the VRH mechanism. The absence of influence of dislocation-clusters on the I-V characteristics shows that more than the number of dislocations at the cluster cores, the critical parameter impacting the leakage is the total number of dislocations within the diodes. The number of dislocations is estimated at 200 in the 100 µm² area occupied by the cluster cores, and it is smaller than the number of other dislocations randomly present within the diode area.

Under reverse bias, more leaky diodes are found on substrates having higher dislocation density and for diodes having diameters larger than 100 µm. Such behavior may be induced by distinctive active defects with density in the range of 10^4 cm^{-2}, which is significantly smaller than the mean dislocation density. Since larger reverse leakage is more likely to appear for the GaN layer with higher mean dislocation density, we suppose that peculiar dislocations may be responsible. Such active defects should be quite randomly located but remain to be clearly identified. Finally, electric field crowding at the periphery of the diodes prevents the study beyond 100 V. Schottky barrier diodes with field plates, and lower n-

doping levels should be studied to evidence any electrical activity of defects under more significant bias.

Supplementary Data

See supplementary data for access to other experimental evidence of the absence of influence of dislocation-clusters on the reverse leakage current.

Acknowledgements

This work was supported by the technology facility network RENATECH and the French National Research Agency (ANR) through the project SCHOGaN and the "Investissements d'Avenir" program GaNeX (ANR-11-LABX-0014). The authors thank Vincent Gelly (SGL) for his help for CL experiments and for fruitful discussions. The authors also thank Prof. Borge Vinter for the helpful reading of the manuscript.

References

[1] F. Roccaforte, P. Fiorenza, R. L. Nigro, F. Giannazzo, G. Greco, *Riv Nuovo Cimento* **2018**, *41*, 625.

[2] A. Lidow, *GaN Transistors for Efficient Power Conversion*, Wiley, Hoboken, NJ **2020**.

[3] C. D. Lee, A. Sagar, R. M. Feenstra, W. L. Sarney, L. Salamanca-Riba, J. W. P. Hsu, *Phys. Status. Solidi A.* **2001**, *188*, 595.

[4] A. Krost, A. Dadgar, *Mater. Sci. Eng. B***. 2002**, *93*, 77.

[5] Y. Saitoh, K. Sumiyoshi, M. Okada, T. Horii, T. Miyazaki, H. Shimoi, M. Ueno, K. Katayama, M. Kiyama, T. Nakamura, *Appl. Phys. Express* **2010**, *3*, 081001.

[6] N. Tanaka, K. Hasegawa, K. Yasunishi, N. Murakami, T. Oka, *Appl. Phys. Express* **2015**, *8*, 071001.

[7] A. M. Ozbek, B. J. Baliga, *IEEE Electron Device Lett.* **2011**, *32*, 300.

[8] T. Kachi, *Jpn. J. Appl. Phys.* **2014**, *53*, 100210.

[9] P. Kruszewski, P. Prystawko, M. Grabowski, T. Sochacki, A. Sidor, M. Bockowski, J. Jasinski, L. Lukasiak, R. Kisiel, M. Leszczynski, *Mat. Sci. Semicon. Proc.* **2019**, *96*, 132.

[10] C. Skierbiszewski, P. Perlin, I. Grzegory, Z. R. Wasilewski, M. Siekacz, A. Feduniewicz, P. Wisniewski, J. Borysiuk, P. Prystawko, G. Kamler, T. Suski, S. Porowski, *Semicond. Sci. Technol.* **2005**, *20*, 809.

[11] C. A. Hurni, A. David, M. J. Cich, R. I. Aldaz, B. Ellis, K. Huang, A. Tyagi, R. A. DeLille, M. D. Craven, F. M. Steranka, M. R. Krames, *Appl. Phys. Lett.* **2015**, *106*, 031101.

[12] https://www.lumilog.com/.

[13] D. Gogova, H. Larsson, A. Kasic, G. R. Yazdi, I. Ivanov, R. Yakimova, B. Monemar, E. Aujol, E. Frayssinet, J.-P. Faurie, B. Beaumont, P.Gibart, *Jpn. J. Appl. Phys.* **2005**, *44*, 3.

[14] T. Florian, D. Martin, P. Vennéguès, N. Grandjean, and P. De Mierry. *Appl. Phys. Lett.* **2016**, 109, 082101.

[15] I. C. Kizilyalli, P. Bui-Quang, D. Disney, H. Bhatia, O. Aktas, *Microelectronics Reliab.* **2015**, *55*, 1654.

[16] J. C. Gallagher, T. J. Anderson, L. E. Luna, A. D. Koehler, J. K. Hite, N. A. Mahadik, K. D. Hobart, F. J. Kub, *J. Cryst. Growth.* **2019**, *506*, 178.

[17] J. K. Hite, T. J. Anderson, L. E. Luna, J. C. Gallagher, M. A. Mastro, J. A. Freitas, C. R. Eddy Jr, *J. Cryst. Growth* **2018**, *498*, 352.

[18] H. Fujikura, K. Hayashi, F. Horikiri, Y. Narita, T. Konno, T. Yoshida, H. Ohta, T. Mishima, *Appl. Phys. Express* **2018**, *11*, 045502.

[19] L. Sang, B. Ren, M. Sumiya, M. Liao, Y. Koide, A. Tanaka, Y. Cho, Y. Harada, T. Nabatame, T. Sekiguchi, S. Usami, Y. Honda, H. Amano, *Appl. Phys. Lett.* **2017**, *111*, 122102.

[20] S. Usami, Y. Ando, A. Tanaka, K. Nagamatsu, M. Deki, M. Kushimoto, S. Nitta, Y. Honda, H. Amano, Y. Sugawara, Y.-Z. Yao, Y. Ishikawa, *Appl. Phys. Lett.* **2018.** *112*, 182106.

[21] Z. Bian, T. Zhang, J. Zhang, S. Zhao, H. Zhou, J. Xue, X. Duan, Y. Zhang, J. Chen, K. Dang, J. Ning, Y. Hao, *Appl. Phys. Express* **2019**, *12*, 084004.

[22] M.-R. Irekti, M. Lesecq, N. Defrance, E. Okada, E. Frayssinet, Y. Cordier, J.-G. Tartarin and J.-C. De Jaeger, *Semicond. Sci. Technol.* **2019**. 34, 12LT01.

[23] M. Khoury, A. Courville, B. Poulet, M. Teisseire, E. Beraudo, M. J. Rashid, E. Frayssinet, B. Damilano, F. Semond, O. Tottereau and P. Vennéguès, Semicond. Sci. Tech. **2013**, 28, 035006.

[24] D. K. Schroder, *Semiconductor material and device characterization*, Wiley, Hoboken, NJ **2006**, Ch. 3.

[25] S. M. Sze, *Physics of Semiconductor Devices*, 2nd ed. Wiley, New York, **2006**, Ch. 5.

[26] H. Hasegawa and S. Oyama, *J. Vac. Sci. Technol.* B **2002**, *20*, 1647.

[27] J. W. P. Hsu, M. J. Manfra, D. V. Lang, S. Richter, S. N. G. Chu, A. M. Sergent, R. N. Kleiman, L. N. Pfeiffer, R. J. Molnar, *Appl. Phys. Lett.* **2001**, *78*, 1685.

[28] H. Yamada, H. Chonan, T. Takahashi, M. Shimizu, *Phys. Status Solidi A.* **2018**, *215*, 1700362.

[29] Y. Beggah, D. E. Mekki, N. Tabet and R. J. Tarento, *Solid-State Electronics.* **1998**, 42, 379.

[30] A.P. Zhang, G. Dang, F. Ren, J. Han, H. Cho, S.J. Pearton, J.-I. Chyi, T.-E. Nee, C.M. Lee, C.C. Chuo, S.N.G. Chu, *Solid-State Electronics.* **2000**, 44, 1157.

[31] E. J. Miller, E. T. Yu, P. Waltereit, and J. S. Speck, *Appl. Phys. Lett.* **2004**, 84, 535.

[32] Y. Zhang, H.-Y. Wong, M. Sun, S. Joglekar, L. Yu, N. A. Braga, R. V. Mickevicius, and T. Palacios, *2015 IEEE International Electron Devices Meeting (IEDM).* **2015**, Washington, DC, pp. 35.1.1-35.1.4.

[33] B. Rackauskas, M.J. Uren, T. Kachi, M. Kuball, *Microelectronics Reliab.* **2019**, *95*, 48.

[34] Y. Sun, X. Kang, Y. Zheng, J. Lu, X. Tian, K. Wei, H. Wu, W. Wang, X.Liu and G. Zhang, *Electronics* **2019**, 8, 575.

[35] J. Bajaj, L. O. Bubulac, P. R. Newman, W. E. Tennant, and P. M. Raccah, *J. Vac. Sci. Technol. A*. **1987**, 5, 3186.

[36] B. Chen, J. Chen, T. Sekiguchi, T. Ohyanagi, H. Matsuhata, A. Kinoshita, H. Okumura, and F. Fabbri, *Appl. Phys. Lett.* **2008**, 93, 033514.